Characterization of quaternary AlInGaN epilayers and polarization-reduced InGaN/AlInGaN MQW grown by MOCVD

Liu Naixin(刘乃鑫)†, Wang Junxi(王军喜), Yan Jianchang(闫建昌), Liu Zhe(刘喆), Ruan Jun(阮军), and Li Jinmin(李晋闽)

(Institute of Semiconductors, Chinese Academy of Sciences, Beijing 100083, China)

Abstract: We have demonstrated the growth of quaternary AlInGaN compounds at different growth temperatures and pressures with metalorganic chemical vapor deposition (MOCVD). The optical properties of the samples have been investigated by photoluminescence (PL) at different temperatures. The results show that the sample grown at higher temperature (850 °C) exhibits the best optical quality for its sharp band edge luminescence and weak yellow luminescence. The AlInGaN exhibited three-dimensional (3D) growth mode at higher pressure. The band edge emission almost disappeared. With the optimization of AlInGaN growth parameters, we replaced the traditional barrier in InGaN/GaN multiple quantum wells (MQWs) with AlInGaN barriers. The peak wavelength for the InGaN/AlInGaN-MQW based light emitting diodes (LEDs) was very stable at various injection current levels because of the polarization-matched InGaN/AlInGaN MQWs.

Key words: AlInGaN; UV-LEDs; MOCVD
DOI: 10.1088/1674-4926/30/11/113003 **PACC:** 7865P; 7280E; 7840G

1. Introduction

Ultraviolet LEDs based on wide band gap III-nitride compound semiconductors have attracted the attention of researchers because of their potential applications, especially for solid state white lighting and detection of biological/chemical agents. The most promising materials as active layers for such UV emitters are AlGaN ternary. However, AlGaN shows a strong piezoelectric field[1] and a spontaneous polarization effect[2], which decreases the radiative efficiency.

Alloys of GaN with InN and AlN can be prepared covering the spectral range from red to vacuum UV (0.7 to 6.2 eV). Such a band gap engineering approach with quaternary alloys allows the independent adjustment of strain and the band offset to realize nearly zero internal field in InGaN/AlInGaN MQW structure[3,4].

By introducing In into AlGaN, a similar effect to that obtained in InGaN-based emitters is expected for quaternary AlInGaN. Enhanced luminescence in quaternary AlInGaN with an In-localization effect has been reported by several authors[5–7].

Although AlInGaN is a promising material, growth of the quaternary alloy is a challenging task due to the different bond lengths, decomposition temperature of the binary compounds and desorption of the growing species. Furthermore, the effects of composition pulling and strain in the layer become dominant with epilayer thickness. This can lead to the generation of V-shaped pits on the epilayer surface giving rise to varying surface morphologies.

In this paper, AlInGaN quaternary alloys were grown with different growth temperatures and reactor pressures. PL was used to study the optical properties of AlInGaN quaternary epilayers. The surface morphology of AlInGaN quaternary alloy was observed using atomic force microscopy (AFM). Rutherford backscattering (RBS) was used to calculate the In and Al contents. The effect of growth temperature and reactor pressure on the optical and morphological properties of AlInGaN quaternary alloy was discussed. Based on the optimization of growth parameters, we realized polarization-matched InGaN/AlInGaN-MQW based LEDs, which emit stable wavelength at various injection current levels.

2. Experimental procedure

The quaternary AlInGaN epilayers were grown by low pressure MOCVD on sapphire (0001) substrates. A low-temperature GaN of 30 nm was first grown as the buffer layer on sapphire followed by an undoped high-temperature GaN layer of 3 μm. On this template, quaternary epilayers of 300 nm were grown at a temperature between 810 to 850 °C. The reactor pressure of AlInGaN was varied between 50 and 200 Torr.

Ammonia (NH3), trimethylaluminum (TMAl), trimethylgallium (TMGa) and trimethylindium (TMIn) were used as precursors. N_2 was used as the carrier gas. The fluxes of the constituent precursors remained constant during the growth.

RBS measurements were performed with a beam of 2 × 1.7 MeV +He ions. The 325 nm line of an He–Cd laser was used as an exciting source for the PL measurements.

† Corresponding author. Email: nxliu@semi.ac.cn
Received 23 March 2009, revised manuscript received 19 June 2009

Table 1. Sample specifications.

Sample	Pressure (Torr)	Temperature (°C)	Composition		FWHM of PL at RT (meV)	AFM RMS of 5×5 μm^2 (nm)
			In (%)	Al (%)		
A	50	850	1	10	30.9	1.03
B	50	830	1.5	10.5	66.1	1.41
C	50	810	3.5	10.5	240	2.0
D	100	850	9.6	10	–	6.13
E	200	850	16.1	10	–	13.3

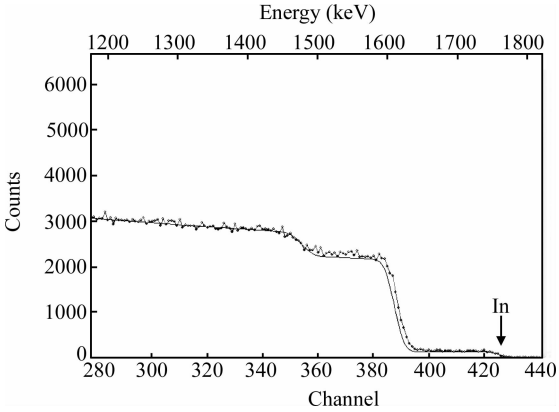

Fig. 1. Random and simulated RBS spectra from sample A.

X-ray diffraction (XRD) was carried out on Bede D1. A tapping mode AFM (Vecco D3100) was used to obtain the AFM images. The observed area was 2×2 μm^2. Some parameters of the samples are listed in Table 1.

In principle, the composition of ternary alloy can be determined by XRD using Vegard's law assuming that the layers are fully relaxed[8]. However, there are 2 variables, x (Al content) and y (In content), in quaternary AlInGaN alloys. Alternatively, the x and y values can also be determined by PL and XRD measurement using the simultaneous equations:

$$\boldsymbol{a}[\mathrm{Al}_x\mathrm{In}_y\mathrm{Ga}_{1-x-y}N] = x\boldsymbol{a}_{\mathrm{AlN}} + y\boldsymbol{a}_{\mathrm{InN}} + (1-x-y)\boldsymbol{a}_{\mathrm{GaN}}, \quad (1)$$

$$E_{\mathrm{g}}[\mathrm{Al}_x\mathrm{In}_y\mathrm{Ga}_{1-x-y}N] = xE_{\mathrm{g}}(\mathrm{AlN}) + yE_{\mathrm{g}}(\mathrm{InN}) + (1-x-y)E_{\mathrm{g}}(\mathrm{GaN}). \quad (2)$$

However, the bowing effects are not included in Eq. (2) since no data is available for the energy gap of AlInGaN quaternary alloys. So the composition of quaternary AlInGaN deduced using this approach is also questionable. On the other hand, RBS is a reliable method which can determine the composition of a quaternary alloy directly without the above-mentioned problems. The compositions of all samples as listed in Table 1 were determined by RBS measurement. Figure 1 shows an RBS random spectrum obtained from sample A. With the simulation by SIMNRA (the simulation software used to analyze the RBS spectra), the In and Al compositions of sample A are respectively 1% and 10%. The ratio of aligned to random yields for the reaction region (300–360 channels) is 2.2%, which confirms the good crystalline quality.

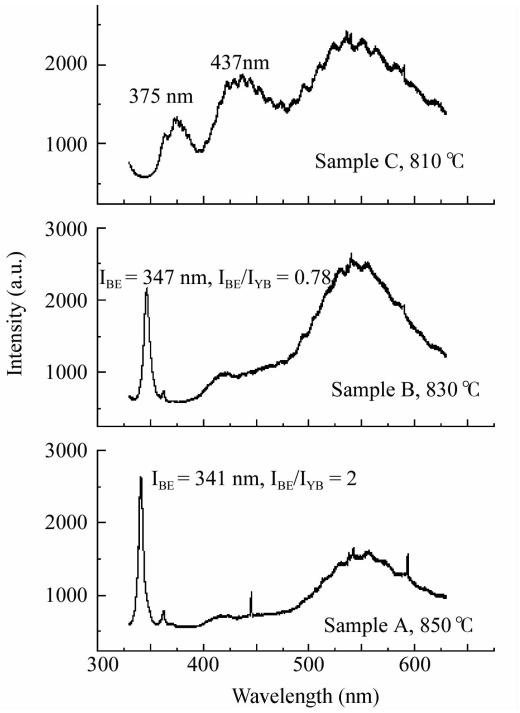

Fig. 2. PL spectra of AlInGaN grown at different temperatures.

3. Results and discussion

3.1. Growth temperature

Figure 2 shows the room temperature PL spectra of the AlInGaN quaternary alloy grown at different temperatures. It is worth noting that the sample grown at a lower temperature exhibits not only band edge emission (I_{BE}) and yellow band emission (I_{YB}) but also broad emission at about 440 nm (I_{abnormal}). The excitation intensity dependent PL experiments illustrate that the abnormal broad peak saturates at high excitation intensity and the peak ratio ($I_{\mathrm{abnormal}}/I_{\mathrm{BE}}$) decreases as the excitation intensity increases. This behavior is a typical footprint of the defects. Thus a lower growth temperature leads to more defects. Enhanced luminescence in quaternary AlInGaN with a higher In content has been found because of the In-segregation effect and the In-localization effect[5–7]. However, sample A with a lower indium content exhibits stronger and narrower band edge emission. Meanwhile, the abnormal broad peak was suppressed significantly in this sample. We attribute this phenomenon to two causes: one is due to the composition fluctuation effect, and low indium content AlInGaN can lead to In-segregation. Another is that relative defect emission was

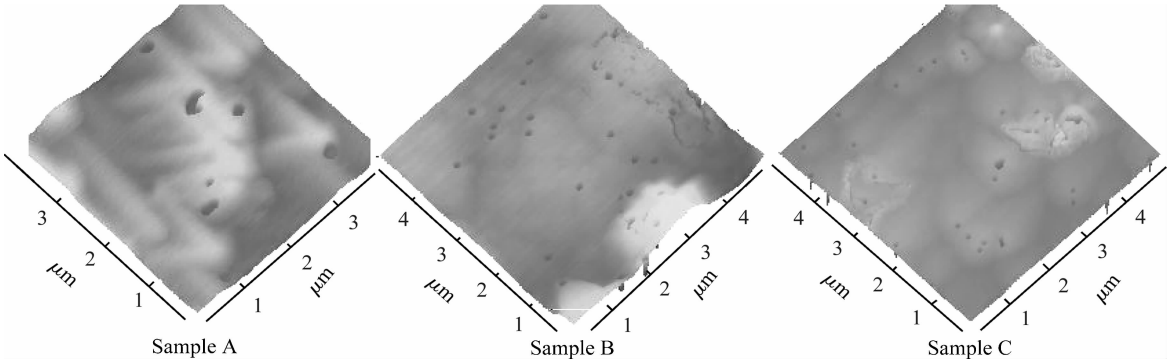

Fig. 3. AFM images of AlInGaN grown at different temperatures.

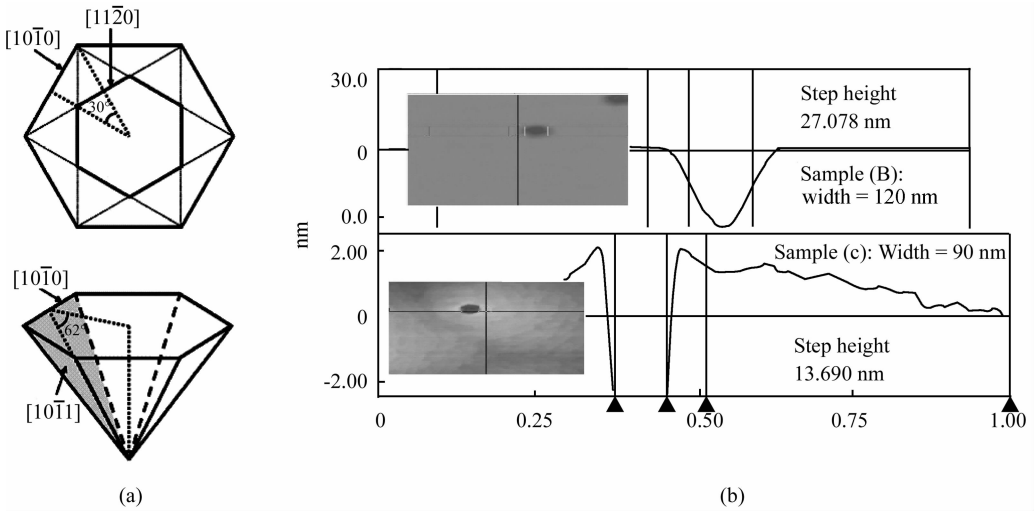

Fig. 4. (a) Structure diagram; (b) Cross-sectional analysis of the V-shaped pits of samples B and C.

suppressed significantly at higher growth temperatures. Based on these reasons, sample A exhibits superior optical properties.

Figure 3 shows AFM images of these AlInGaN epilayers grown at different temperatures. The surface morphologies of these samples show atomic steps besides V-shaped pits. The density of the V-shaped pits in samples A, B, C is respectively 5.6×10^7, 1.2×10^8, and 1.44×10^8 cm^{-2}, and the RMS is respectively 1.03, 1.41, and 2 nm. We conclude that the segregation of indium which happens severely at lower growth temperatures leads to more V-shaped pits and a rougher surface.

A similar morphology to Fig. 3 has previously been reported in InGaN/GaN multiple quantum wells and bulk InGaN film[9, 10]. The V-shaped pits with the structure as shown in Fig. 4(a) in these InGaN epilayers are formed when threading dislocations intersect the epilayer surface. The strain energy induced by the lattice mismatch between InGaN and GaN and the reduction of surface mobility due to the low growth temperature of InGaN are major contributors to pit formation. We suggest that the V-shaped pits in our AlInGaN epilayers have the same formation mechanism due to the similar growth conditions. Indium atoms tend to congregate in the dislocation core areas due to the low growth temperature. Thus local indium segregation may slow down or inhibit crystal growth in this area, which initiates pit formation. These pits in InGaN tend to have a steeper sidewall and an aspect ratio given by the depth-diameter ratio $\sim \sqrt{8/3}$. From the cross-sectional analysis of the V-shaped pits of samples B and C, as depicted in Fig. 4(b), it is observed that the pit filling tends to give rise to truncated V-shaped pits. The depth-diameter ratio of the V-shaped pits in samples B and C is respectively 0.45 and 0.3. From Table 1, the indium composition of sample C is 2.3 times that of sample B. A higher indium content leads to shallower pits by pit filling, so we suggest that these pits were filled by indium related defects.

3.2. Growth pressure

Figure 5 shows the (0002) ω–2θ scan of AlInGaN grown at different pressures. From this figure, we can clearly see that a higher reactor pressure favors indium incorporation. On increasing the growth pressure, the band edge emission intensity of PL was notably decreased, implying a decrease in optical quality as shown in Fig. 6. The origin of the deteriorated optical quality is related to the microstructural properties of the AlInGaN epilayer. The initial stage of the island is grown under reduced atomic mobility because of the big misfit strain energy at the interface grown at high pressure. Subsequently, each island with a different stacking order meets in the continuous growth and a lot of stacking faults are generated by stacking mismatches at the boundaries of islands.

Figure 7 shows AFM images of the AlInGaN epilayers

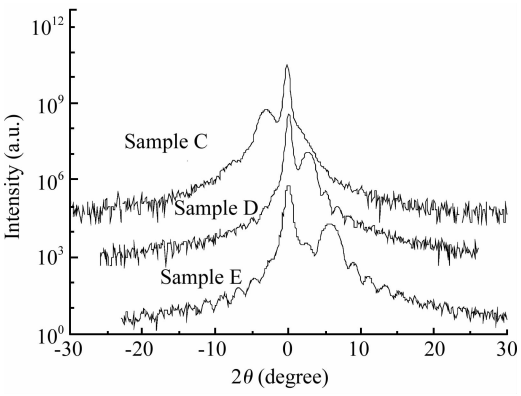

Fig. 5. XRD (0002) ω–2θ scan of AlInGaN grown at different pressures.

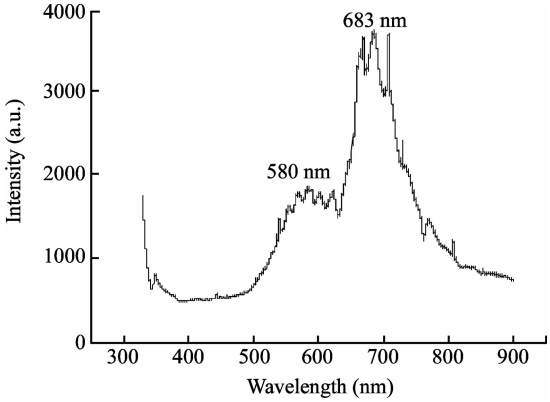

Fig. 6. PL spectrum of AlInGaN grown at higher pressures for sample E.

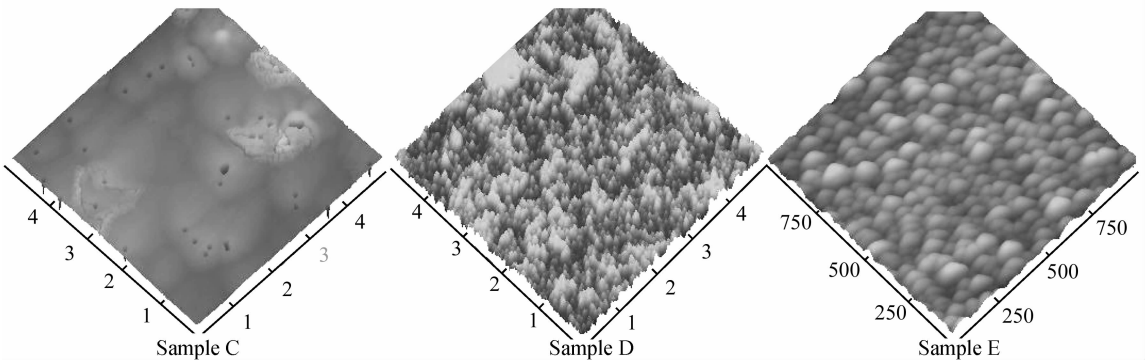

Fig. 7. AFM images of AlInGaN grown at different pressures.

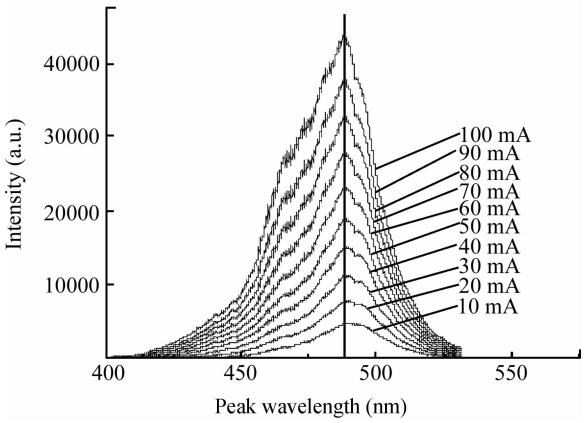

Fig. 8. EL spectra of InGaN/AlInGaN LED at 10–100 injection current.

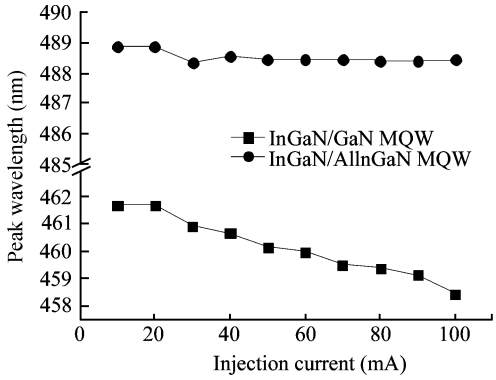

Fig. 9. Peak wavelength of EL at different injection current levels in InGaN/GaN and InGaN/AlInGaN-MQW based LEDs.

grown at different pressures. The samples grown under high pressures show a 3D growth mode, the sample roughness increases rapidly and the V-shaped pits disappear.

3.3. AlInGaN/InGaN MQWs

Previous studies have indicated that electron leakage from the active region is enhanced by sheet charges at heterointerfaces that result from polarization mismatch between GaN (barriers) and InGaN (wells) in a conventional LED active region[11]. Our quaternary AlInGaN appears to have the possibility of reducing polarization fields as a consequence of the improved polarization matching between InGaN (wells) and AlGaInN (barriers). According to the above investigation of the AlInGaN bulk layer, we adopted the growth parameters of sample A to replace the barrier in traditional InGaN/GaN-MQW based LEDs. Meanwhile, we adjust the composition to $Al_{0.05}In_{0.05}Ga_{0.9}N$ to reduce the lattice mismatch. From the EL results performed at various injection current levels and consistent with an increase in the sheet charge magnitude, the shift in peak wavelength with increasing current is very small as shown in Fig. 8. We also measure the EL spectra of traditional InGaN/GaN-MQW based LEDs as a benchmark. The peak position significantly blue-shifts as the driving current increases due to the high polarization fields. However, we could not find any shift to shorter wavelengths in our InGaN/AlInGaN-MQW based LEDs as the current was increased, as shown in Fig. 9.

4. Conclusions

In summary, the optical properties of higher temperature grown quaternary AlInGaN epilayers were superior. The segregation of indium which happens at lower growth temperatures leads to more V-shaped pits and a rougher surface. The surface morphology of the AlInGaN quaternary epilayers deteriorated rapidly with increasing growth pressure. The higher growth pressure leads to 3D growth mode. Furthermore, we have demonstrated InGaN MQWs with polarization-matched quaternary AlInGaN barriers rather than the conventional GaN barriers. The peak wavelength for the InGaN/AlInGaN-MQW based LED is very stable at various injection current levels.

References

[1] Akasaki L, Sota S, Sakai H, et al. Shortest wavelength semiconductor laser diode. Electron Lett, 1996, 32: 1105

[2] Nakamura S, Senoh S, Nagahama S, et al. InGaN-based multi-quantum well structure laser diodes. Jpn J Appl Phys, 1996, 35(Part 2): L74

[3] Knauer A, Wenzel H, Kolbe T, et al. Effect of the barrier composition on the polarization fields in near UV InGaN light emitting diodes. Appl Phys Lett, 2008, 92: 191912

[4] Schubert M F, Xu J, Kim J K, et al. Polarization-matched GaInN/AlGaInN multi-quantum-well light-emitting diodes with reduced efficiency droop. Appl Phys Lett, 2008, 93: 041102

[5] Hirayama H, Kinoshita A, Yamabi T, et al. Marked enhancement of 320–360 nm ultraviolet emission in quaternary $In_xAlyGa_{1-x-y}N$ with In-segregation effect. Appl Phys Lett, 2002, 80: 207

[6] Chitnis A, Kumar A, Shatalov M, et al. High-quality p–n junctions with quaternary AlInGaN/InGaN quantum wells. Appl Phys Lett, 2000, 77: 3800

[7] Ryu M Y, Chen C Q, Kuokstis E, et al. Luminescence mechanisms in quaternary $Al_xIn_yGa_{1-x-y}N$ materials. Appl Phys Lett, 2002, 80: 3730

[8] Nakamura S, Faso G. The blue laser diode. Berlin: Springer-Verlag, 1997

[9] Chen Y, Takeuchi T, Amano H, et al. Pit formation in GaInN quantum wells. Appl Phys Lett, 1998, 72: 710

[10] Kim I H, Park H S, Park Y J, et al. Formation of V-shaped pits in InGaN/GaN multiquantum wells and bulk InGaN films. Appl Phys Lett, 1998, 73: 1634

[11] Kim M H, Schubert M F, Dai Q, et al. Origin of efficiency drop in GaN-based light-emitting diodes. Appl Phys Lett, 2007, 91: 183507